SILVER NANOPARTICLE DECORATED 2D-$MoSe_2$ NANOSHEETS FOR EXPLORATION OF OPTICAL PROPERTIES

Shahnaz Shabnam*[1] and Gazi Ameen Ahmed[1]

[1]*Department of Physics, Tezpur University, Napaam -784028, Assam, India*

*Corresponding Author: shahnazshabnam07@gmail.com

(Received 26 September 2025; revised 6 November 2025; accepted 13 December 2025; published 1 August 2026)

Abstract: The present work illustrates the synthesis of a transition metal dichalcogenide material (TMDC), $MoSe_2$ and its composite with Silver (Ag) nanoparticles, employing the liquid phase exfoliation method through a sonication process. The synthesized $MoSe_2$ nanosheets and $MoSe_2$–Ag nanocomposite exhibits synergistically enhanced optical properties compared to that of bulk $MoSe_2$. The optical bandgap comparison of $MoSe_2$, $MoSe_2$-Ag was investigated using UV-Vis Spectroscopy. The corresponding nanostructures were determined by Scanning Electron Microscopy (SEM), Field Emission Scanning Electron Microscopy (FESEM), X-Ray diffraction (XRD), Raman spectroscopy.

Keywords: Transition metal dichalcogenide material (TMDC); Molybdenum Diselenide ($MoSe_2$); Bandgap

PACS: 78.20.-e 78.90.+t

1 Introduction

Two-dimensional materials are regarded as highly promising candidates for next-generation applications in electronics and optoelectronics [1]. Among various 2D materials, transition metal dichalcogenides (TMDCs) (MoS_2, $MoSe_2$, $MoTe_2$, WS_2, and WSe_2) have attracted extensive research attention owing to their distinctive optical, electrical, catalytic, and mechanical properties 2,3. Molybdenum Diselenide ($MoSe_2$), a representative member of the TMDC family, is a layered 2D material that has gained significant interest due to its large surface area, tunable bandgap, etc., making it a potential candidate for applications in optoelectronic devices, energy storage, catalysis, sensing, etc. [2, 3]. Bulk $MoSe_2$ has indirect band gap of 1.1 eV, which changes to direct band gap after exfoliation. The monolayer and few layers of $MoSe_2$ nanosheets exhibit band gaps of about 1.41 eV and (1.5-1.6 eV) respectively [4]. This wide band gap semiconductor is characterized by its excellent optical transparency, adjustable carrier concentration, and tunable electrical conductivity [5]. These characteristics make $MoSe_2$ highly attractive for application in optoelectronics, photovoltaics, photocatalysis, photodetectors, and chemical sensing [6, 7]. In its monolayer form, $MoSe_2$ exhibits a direct bandgap that enhances light- matter interactions and promotes strong absorption within the UV–visible region [8, 9]. Furthermore, its excellent thermal and chemical stability ensures reliable performance under harsh environmental conditions [10]. These combined features establish $MoSe_2$ as a promising candidate for advanced optoelectronic applications [11]. To further enhance the optical and electrical properties of $MoSe_2$, researchers have employed various innovative strategies such as metal or non-metal doping, layer-number control, heterostructure formation, strain engineering, plasmonic nanoparticle decoration, and surface functionalization [12, 13]. Among these approaches, hybridization with plasmonic nanostructures such as silver (Ag), gold (Au), and copper (Cu) nanoparticles has proven particularly effective due to their localized surface plasmon resonance (LSPR) effects, strong light-scattering ability, and high electrical conductivity [14]. When decorated on 2D MoSe2 nanosheets, plasmonic nanoparticle can induce synergistic interactions that modulate the band structure, promote charge transfer, and enhance light absorption across a broader

spectral range. These hybrid effects are expected to significantly boost the performance of $MoSe_2$-based systems in optoelectronic devices, energy storage, optical detection platforms, and photocatalytic application.

In this this work we report a facile sonication-assisted method for the decoration of Ag nanoparticle onto $MoSe_2$ nanosheets to form $MoSe_2$-Ag nanocomposite. The synthesized hybrid system was systematically investigated to study the synergistic modulation of the optical bandgap and the enhancement of the optical properties of $MoSe_2$ nanosheets.

2 Materials and methods

2.1 Materials

Bulk $MoSe_2$(99.9%) was purchased from Thermo Scientific, N- Methyl-2-pyrolidone (NMP) was purchased from merck. Silver Nitrate ($AgNo_3$, 98.5%) was purchased from Loba Chemie and Sodium Borohydride ($NaBH_4$) from SRL.

2.2 Synthesis

$MoSe_2$ nanosheets were exfoliated from bulk $MoSe_2$ using Liquid Phase Exfoliation (LPE) method. It is an ultrasound-assisted technique where cavitation occurs and breaks the Van Der Walls cohesive forces between the layers to form exfoliated structures [15]. For the exfoliation of $MoSe_2$, a bath sonicator with an ultrasonic power 60 W was employed. Twenty milligrams of bulk $MoSe_2$ were dispersed in N-methyl-2-pyrrolidone (NMP) solvent followed by stirring and sonicated for 8 hours. The dispersion was further centrifuged at 7000 rpm for 20 min to separate the exfoliated nanosheets from the sediment. The sediment was washed several times and dried, after that added in DI water for further use.

The Silver nanoparticles (AgNPs) were synthesized from $AgNO_3$ by a chemical reduction method using Sodium Borohydride (NaBH4) as the reducing agent. Ten milliliters of 1 mM $AgNO_3$ solution were added drop wise to 30ml of 2mM freshly prepared $NaBH_4$. After complete reduction, a light brown colour Ag nanoparticle was obtained. To synthesize $MoSe_2$-Ag nanocomposite 20ml of exfoliated $MoSe_2$ dispersion and 20 ml of Ag nanoparticle suspension were mixed and sonicated for 3 hours to ensure uniform decoration of AgNPs on the $MoSe_2$ nanosheets.

3 Results and Discussion

The morphology of the exfoliated $MoSe_2$ nanosheets was examined using FESEM (JEOL). The sheets like layered structures were observed from the FESEM image (Fig. 1.a). The crystalline structure of bulk $MoSe_2$, exfoliated $MoSe_2$ and Ag-decorated $MoSe_2$ nanosheets ($MoSe_2$-Ag) were studied by P-XRD (BRUKER AXS). The diffraction peaks of bulk $MoSe_2$ (Fig. 1.c) are well indexed to the hexagonal phase (JCPDS card no. 29-0914), with prominent reflections corresponding to the (002), (004), (100), (103), (105), and (110) planes. These sharp and intense peaks confirm the high crystallinity of the bulk material. Some peaks are absent in exfoliated $MoSe_2$ which were present in bulk indicating a reduction in stacking order and the formation of few-layered nanosheets. Distinct Ag peaks are not observed in the $MoSe_2$–Ag nanocomposite, likely due to low Ag loading below the XRD detection limit or the formation of poorly crystalline Ag nanoparticles that produce weak, broadened diffraction signals. The energy dispersive X-ray spectroscopy (EDX) has been performed to identify the elemental composition of Mo, Se, and Ag (Fig. 1.d). The EDX spectra and the elemental mapping of Mo, Ag, and Se confirm the formation of $MoSe_2$-Ag nanocomposites. The smaller peaks below 1 keV are likely due to light elements such as carbon (C), oxygen (O), or nitrogen (N). These are commonly observed in EDX spectra and can originate from the sample environment, carbon tape, or minor surface contamination. The Raman spectroscopy shows the typical peaks of $MoSe_2$ nanosheets at 242 cm^{-1} and 289 cm^{-1}, which corresponds to the out-of-plane A_{1g} mode, in-plane E^1_{2g} mode [16]. Although the intensity of A_{1g} decreases in exfoliated nanosheets compared to the bulk $MoSe_2$, it increases again after incorporation of Ag nanoparticles. The optical properties of bulk $MoSe_2$, exfoliated $MoSe_2$ nanosheets and Ag-decorated $MoSe_2$ ($MoSe_2$-Ag) nanocomposite were investigated using UV–Vis spectroscopy, as shown in Fig 2. The two noticeable excitonic peaks, B($\sim$730nm) and A($\sim$836nm) are observed for bulk $MoSe_2$ which redshift to $\sim$706 and $\sim$807, respectively, for exfoliated $MoSe_2$. These arise from valence-band splitting caused by spin–orbit coupling, confirming the formation of few-layer 2H-phase $MoSe_2$ nanosheets [17]. Pristine $MoSe_2$ exhibits broad absorption across the UV–visible region, characteristic of its semiconducting nature

and excitonic transitions associated with layered TMDCs. After Ag decoration, the $MoSe_2$-Ag nanocomposite exhibits enhanced absorption intensity, particularly in the visible region, along with a more pronounced feature around ∼420 nm. This enhancement is attributed to the localized surface plasmon resonance (LSPR) effect of Ag nanoparticles, which facilitates stronger light–matter interactions and improves photon harvesting. The increased absorbance also indicates effective electronic coupling between Ag nanoparticles and $MoSe_2$ nanosheets, promoting charge transfer and broadening the optical response. The optical bandgap was estimated (Fig. 2c-e) using the

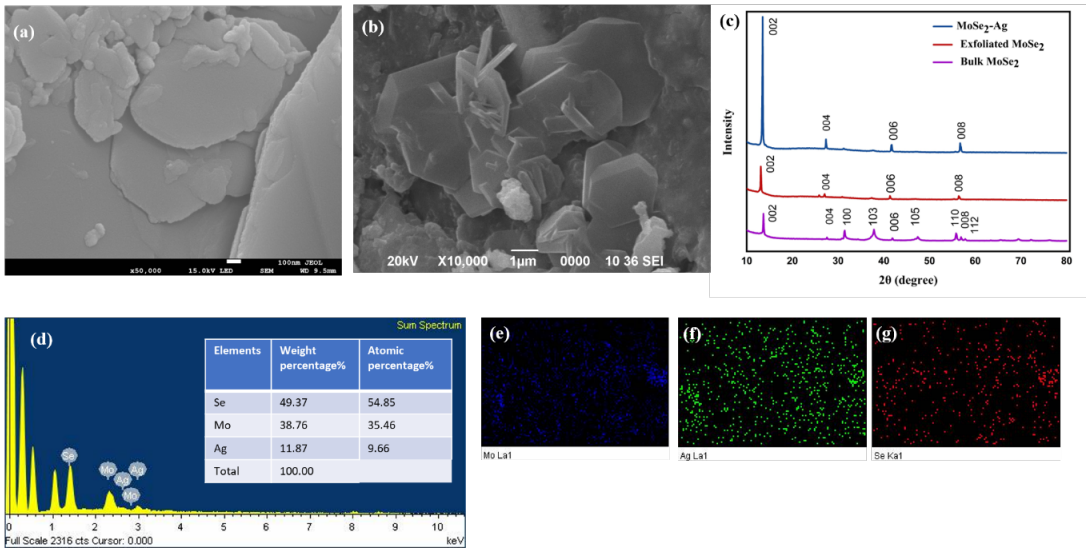

Figure 1: (a) FESEM image of exfoliated $MoSe_2$ nanosheets (b) SEM image of $MoSe_2$-Ag nanocomposite (c) XRD Spectra (d) EDX Spectra of $MoSe_2$-Ag nanocomposite (e)-(g) elemental mapping of Mo, Ag, Se respectively

Tauc relation

$$(\alpha h\nu)^x = A(h\nu - E_g) \tag{1}$$

Where $\alpha, h\nu, A, E_g$ are the absorption coefficient, photon energy, proportionality constant, and optical band gap, respectively. The value of x is $\frac{1}{2}$ for indirect transitions and 2 for direct allowed transitions. For bulk $MoSe_2$, the indirect band was estimated to be approximately 1.2eV, which increases to a direct bandgap of about 2.2 eV for exfoliated $MoSe_2$. Meanwhile, the $MoSe_2$-Ag nanocomposite exhibited a slightly reduced band gap of around 2.0 eV compared to pristine $MoSe_2$. This narrowing of the band gap upon Ag decoration can be attributed to strong interfacial interactions between $MoSe_2$ nanosheets and Ag nanoparticles. These interactions introduce additional electronic states and facilitate charge transfer, effectively lowering the transition energy. The decrease in band gap, along with enhanced optical absorption, indicates that Ag decoration successfully modifies the electronic structure of $MoSe_2$, enabling more efficient utilization of the visible spectrum. Such band gap engineering is advantageous for applications in optoelectronics, photocatalysis, and colorimetric sensing, where broad spectral absorption and efficient charge transport are crucial.

4 Conclusion

In this study, $MoSe_2$ nanosheets were successfully synthesized using the liquid-phase exfoliation (LPE) technique. Silver nanoparticles were incorporated through a sonication-assisted method to fabricate $MoSe_2$–Ag nanocomposites, resulting in a significant enhancement of their optical properties. The XRD confirmed the formation of few-layer $MoSe_2$ with uniformly dispersed AgNPs. UV–Vis spectroscopy revealed enhanced optical absorption due to the plasmonic effect of Ag, while Tauc analysis indicated a reduction in the optical bandgap from ∼2.2 eV to ∼2.0 eV after Ag incorporation. These findings demonstrate that Ag decoration effectively enhances light harvesting and tunes the electronic structure of $MoSe_2$, making the nanocomposite a promising material for optoelectronic, photocatalytic, and sensing applications.

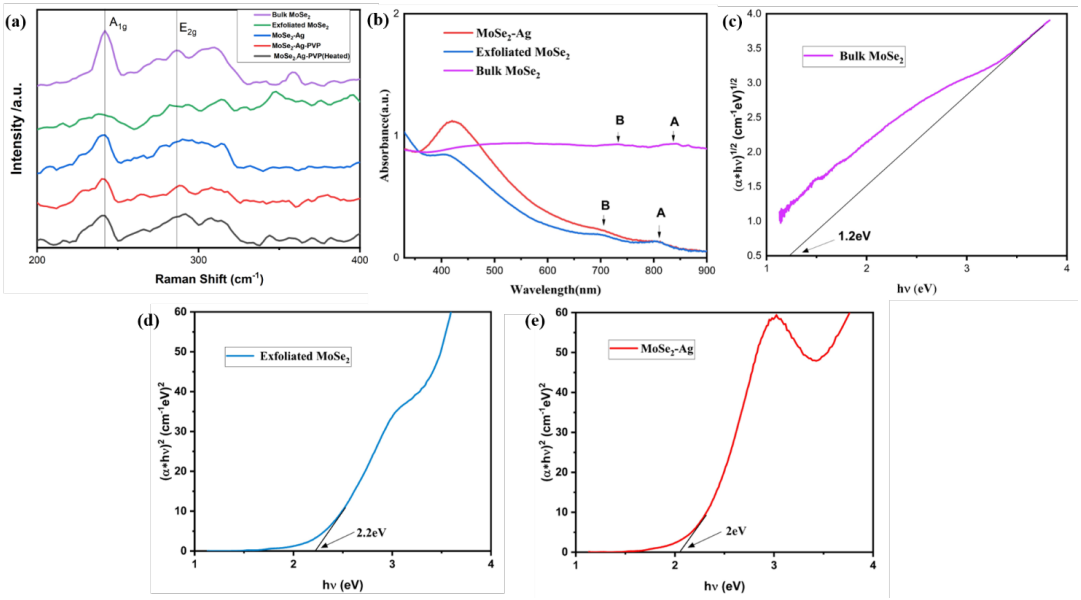

Figure 2: (a) Raman Spectroscopy, (b) UV-Vis Spectroscopy Tauc plot for (c) bulk $MoSe_2$ (indirect band gap) (d) exfoliated $MoSe_2$ (e) $MoSe_2$-Ag nanocomposite

Acknowledgements:

Authors would like to acknowledge SAIC Tezpur University for providing XRD and FESEM, EDX facilities. The authors also thank Dr. Pabitra Nath for providing access to the Raman Spectrometer. The authors would also like to give thanks to Dr. Rajib Biswas for providing the UV-Visible Spectrophotometer facility.

References

[1] T. Tan, X. Jiang, C. Wang, B. Yao, and H. Zhang, Adv. Sci. **7**, 2000058 (2020).

[2] A. Ghorai, S. K. Ray, and A. Midya, ACS Appl. Nano Mater. **4**, 2999 (2021).

[3] Z. Dehghani, F. Ostovari, and M. Nadafan, J. Appl. Phys. **131**, 213101 (2022).

[4] A. Arora, K. Nogajewski, M. Molas, M. Koperski, and M. Potemski, Nanoscale **7**, 20769 (2015).

[5] A. Chafai, I. Essaoudi, M. Behloul, A. Ainane, and C. A. Duque, Phys. B: Condens. Matter **651**, 414574 (2023).

[6] F. Zhong, J. Ye, T. He, L. Zhang, *et al.*, Small **17**, 2102855 (2021).

[7] A. Eftekhari, Appl. Mater. Today **8**, 1 (2017).

[8] G. S. Papanai, K. R. Sahoo, S. Gupta, and B. K. Gupta, RSC Advances **12**, 13428 (2022).

[9] F. Creazzo, ACS Applied Materials and Interfaces **17** (2025).

[10] J. Sun, K. Dai, W. Xia, W. Chen, K. Jiang, Y. Li, *et al.*, ACS Omega **6**, 30526 (2021).

[11] B. Babariya, D. Raval, S. K. Gupta, and P. N. Gajjar, Mater. Today Commun. **28**, 102614 (2021).

[12] K. Nam, J. Im, G. H. Han, J. Y. Park, H. Kim, S. Park, S. Yoo, *et al.*, ACS Omega **9**, 21587 (2024).

[13] K. Vasu, O. E. Meiron, A. N. Enyashin, R. Bar-Ziv, and M. Bar-Sadan, J. Phys. Chem. C **123**, 1987 (2018).

[14] J. Wu, Y. Lu, Z. Wu, S. Li, Q. Zhang, Z. Chen, and Q. Liu, Sens. Actuators B: Chem. **261**, 279 (2018).

[15] P. Sriram, A. Manikandan, F. C. Chuang, and Y. L. Chueh, Small **16**, 1904271 (2020).

[16] P. Tonndorf, R. Schmidt, P. Böttger, X. Zhang, J. Börner, A. Liebig, *et al.*, Opt. Express **21**, 4908 (2013).

[17] N. Dong, Y. Li, Y. Feng, S. Zhang, X. Zhang, C. Chang, and J. Wang, Sci. Rep. **5**, 14646 (2015).